



Far-infrared self-continuum absorption of H₂16O and H₂18O (15–500 cm⁻¹)

T.A. Odintsova, M. yu. Tretyakov, A.O. Zibarova, O. Pirali, Pascal Roy, A. Campargue

► To cite this version:

T.A. Odintsova, M. yu. Tretyakov, A.O. Zibarova, O. Pirali, Pascal Roy, et al.. Far-infrared self-continuum absorption of H₂16O and H₂18O (15–500 cm⁻¹). Journal of Quantitative Spectroscopy and Radiative Transfer, 2019, 227, pp.190-200. 10.1016/j.jqsrt.2019.02.012 . hal-02271449

HAL Id: hal-02271449

<https://hal.science/hal-02271449>

Submitted on 22 Oct 2021

HAL is a multi-disciplinary open access archive for the deposit and dissemination of scientific research documents, whether they are published or not. The documents may come from teaching and research institutions in France or abroad, or from public or private research centers.

L'archive ouverte pluridisciplinaire **HAL**, est destinée au dépôt et à la diffusion de documents scientifiques de niveau recherche, publiés ou non, émanant des établissements d'enseignement et de recherche français ou étrangers, des laboratoires publics ou privés.



Distributed under a Creative Commons Attribution - NonCommercial 4.0 International License

Far-infrared self-continuum absorption of H₂¹⁶O and H₂¹⁸O (15-500 cm⁻¹)

T.A. Odintsova¹, M.Yu Tretyakov¹, A.O. Zibarova^{1,2}, O. Pirali^{3,4}, P. Roy³ and A. Campargue^{5*}

¹ Institute of Applied Physics, Russian Academy of Sciences, Nizhniy Novgorod, Russia,

² Lobachevsky State University of Nizhny Novgorod, Nizhny Novgorod, Russia

³ SOLEIL Synchrotron, L'Orme des Merisiers, Saint-Aubin 91192, Gif-Sur-Yvette, France

⁴ Institut des Sciences Moléculaires d'Orsay (ISMO), CNRS, Univ Paris Sud, Université Paris-Saclay, F-91405 Orsay, France

⁵ Univ. Grenoble Alpes, CNRS, LIPhy, 38000 Grenoble, France

Key words: water continuum; far infrared, synchrotron, water dimer; far line wing

*Corresponding author: Alain Campargue (Alain.Campargue@univ-grenoble-alpes.fr)

Abstract

The water vapor continuum absorption is studied in a spectral range covering most of the pure rotational spectrum of water molecule up to 500 cm^{-1} . The continuum absorption was derived from the broad band water vapor spectra recorded by Fourier transform spectrometer equipped with the 151-m multipass gas cell at the AILES beam line of the SOLEIL synchrotron. The coherent ($10\text{-}35\text{ cm}^{-1}$) and standard ($40\text{-}500\text{ cm}^{-1}$) radiation modes of the synchrotron were used. In order to refine the magnitude and clarify the physical origin of the continuum, spectra of the two major water isotopologues, H_2^{16}O and H_2^{18}O , were considered. Recordings at several water vapor pressures were used to check the expected quadratic pressure dependence of the continuum.

The new data extend and supplement previous measurements filling, in particular, the gap between 200 and 350 cm^{-1} , which was never studied before. The H_2^{16}O and H_2^{18}O absorption continua in the range of $50\text{-}650\text{ cm}^{-1}$ show similar frequency dependence and magnitude. In particular, both continua exhibit a clear water dimer spectral signature near 15 cm^{-1} , in good agreement with previous *ab initio* calculations. The present data confirm that the MT-CKD empirical continuum model widely used in atmospheric applications, overestimates importantly the continuum magnitude in the whole range of the rotational band. The observed irregular frequency dependence of the retrieved C_s values is tentatively interpreted as due to uncertainties on the resonance lines of the water monomer spectrum which is subtracted from the recorded spectra. On the basis of spectra simulations, the inadequate description of the line shapes in the range of the intermediate wings (detuning of $5\text{-}10\text{ cm}^{-1}$ from line center) and the uncertainties on the self-broadening coefficients of water monomer lines are identified as possible mechanisms responsible of the observed irregular fluctuations.

1. Introduction

The terahertz spectral region (in particular the 10-650 cm^{-1} interval) offers great potential for astronomy and atmospheric science. The region contains rotational transitions of many minor and major constituents which are significant for atmospheric chemistry and planetary climate. This frequency range covers the major part of the pure rotational band of the water molecule. Although being a minor constituent ($\approx 0.3\%$ of the atmospheric mass), water vapor is the dominant contributor to the atmospheric absorption in this range. In general, the present accuracy of water line parameters (center frequency, intensity and broadening coefficients) presented in spectroscopic database [Gordon2016] fulfills most of the requirements of modern remote sensing experiments. In addition to rotational and rovibrational absorption lines, water vapor exhibits a continuum absorption which has been measured in several infrared regions and in the microwave, but which has been poorly studied in the far IR. Even though the continuum is several orders of magnitude weaker than absorption at the center of absorption lines, its integrated contribution to the total atmospheric absorption is significant and exceeds the contribution of other greenhouse gases, such as CO_2 and CH_4 . Thus, appropriate calculations of radiation balance, modeling of global climate changes and atmosphere remote sensing require accounting for the water vapor continuum. This is confirmed by estimations based on the semi empirical MT-CKD model of the water vapor continuum [Mlawer, 2012; http://rtweb.aer.com/continuum_frame.html], that is widely used to take into account water vapor continuum in radiative transfer codes.

Preliminary test-validation of the MT-CKD self-continuum in the terahertz region [Odintsova2017] revealed a significant overestimation. The MT-CKD model is regularly adjusted to available experimental data. For instance, the latest version (V3.2) was adjusted in the 4.0, 2.1, 1.6 and 1.25 μm windows on the basis of accurate measurements by cavity ring down spectroscopy (CRDS) [Campargue2016, Richard2017, Lechevallier2018]). Nevertheless, these empirical adjustments do not insure satisfactory extrapolation capabilities to other spectral intervals or to different thermodynamic conditions. The still missing development of a physically based model is probably the most appropriate approach. Indeed, in spite a long history [Shine, 2012], the nature of the water vapor continuum remains poorly understood. Detailed discussion of this problem can found, for example, in our recent paper [Serov2017] and references therein.

In this paper, we present new measurements of the water vapor continuum absorption in the range covering most part of the pure rotational band. Similarly to the work presented in [Odintsova2017] in the 15-35 cm^{-1} and 40-200 cm^{-1} intervals, the spectra were recorded at the SOLEIL synchrotron facility using Fourier Transform Spectroscopy (FTS). Here the spectral range is extended up to 500 cm^{-1} and a higher signal to noise is achieved allowing decreasing error bars on the retrieved continuum. In addition, the absorption continuum of the H_2^{18}O isotopologue is investigated for the first time using the same experimental setup. Such isotopic substitution may give key insights on the physical nature of the water continuum.

2. Experiment

The experimental approach is mostly identical to that used in [Odintsova2017]. Briefly, water vapor absorption spectra were recorded at the AILES beamline of the SOLEIL synchrotron using the coherent (15-35 cm^{-1}) and standard (50-500 cm^{-1}) radiation modes and the high resolution Fourier-transform spectrometer (Bruker IFS125-HR) equipped with a multipass White type configuration cell. The total absorption pathlength was 151.75 ± 1.5 m. Spectra were recorded at room temperature 296(2) K. Normal water sample and ^{18}O enriched water sample (97% enrichment from Euristotop) were used. Detailed experimental conditions of the recordings are presented in **Table 1**.

Table 1. Experimental conditions of the recordings (151.75 m path length).

Freq. Range, cm ⁻¹	<i>P</i> , mbar	Resolution, cm ⁻¹	Number of acquisitions
H₂¹⁶O			
15-35	16.00	0.02	1520
	11.03		100
40-650	6.099	0.02	200
	5.495		
	4.999		
	4.000		
	2.995		
	5.993	0.002	380
H₂¹⁸O			
15-35	15.94	0.02	1060
	13.13		1340
40-650	6.018	0.02	200
	5.450		
	5.000		
	4.500		
	3.993		
	3.497		
	2.994		
	1.985		
	3.991	0.002	200
	5.982		

The experiment provides transmitted light power obtained with cell filled with water vapor, $I(\nu)$, or with the cell evacuated, $I_0(\nu)$. The experimental transmittance, $I(\nu)/I_0(\nu)$, can be approximated by $e^{-\alpha(\nu)l} \otimes f_{app}$ where $\alpha(\nu)$ is the total absorption coefficient and f_{app} is the apparatus function of the considered recording. $\alpha(\nu)$ is the sum of the contributions of the monomer resonance lines, α_{res} , and of the continuum, α_{con} :

$$\alpha(\nu) = \alpha_{res}(\nu) + \alpha_{con}(\nu) \quad (1)$$

Considering the smooth frequency dependence of the continuum, the transmittance can be expressed as $e^{-\alpha_{con}(\nu)l} \times e^{-\alpha_{res}(\nu)l} \otimes f_{app}$. The apparatus function includes the effect of the finite spectral resolution and finite field of view which were modeled by a sinc and boxcar function, respectively.

The resonance absorption coefficient was calculated as the sum of lines with parameters taken from the HITRAN database [Gordon2016], except for a number of lines, for which more accurate experimental data on collisional broadening and shifting parameters were preferred [Golubiatnikov2005, Golubiatnikov2006, Golubiatnikov2008, Koshelev2007, Koshelev2011a, Tretyakov2013]:

$$\alpha_{res}(\nu) = \sum_i S_i \Phi_i(\nu), \quad (2)$$

where i is the line index and S_i and $\Phi_i(\nu)$ the corresponding line intensity and normalized line profile, respectively. For the line profile, we used following expression:

$$\Phi(\nu) = \frac{R(\nu)}{\pi} \left(\frac{\Delta\nu_c}{(\nu - \nu_0)^2 + \Delta\nu_c^2} + \frac{\Delta\nu_c}{(\nu + \nu_0)^2 + \Delta\nu_c^2} \right), \quad (3)$$

where, ν_0 is the line center frequency and $\Delta\nu_c$ is the collisional width. $R(\nu)$ is the general expression for the radiation term suggested in [Clough1989]:

$$R(\nu) = \frac{\nu}{\nu_0} \frac{\tanh(h\nu/2kT)}{\tanh(h\nu_0/2kT)}, \quad (4)$$

where k is the Boltzmann constant and T the temperature.

Formulae (3) reduces at low frequencies to the van Vleck-Weisskopf (VVW) line shape, which is usually preferred in the mm-submm wave range, and at high frequencies, to the Lorentz profile which is generally adopted in the infrared. The range under consideration is an intermediate range where specific frequency dependence of $R(\nu)$ should be taken into account. The standard far-wing cut-off at 25 cm^{-1} from the line center [Clough1989] was applied, the $[-25, +25 \text{ cm}^{-1}]$ “plinth” being excluded and thus contributing to the continuum.

In the case of the spectra recorded with highly ^{18}O enriched water vapor, the isotopic composition of the sample was determined from the recorded spectra using a number of unsaturated absorption lines. The following values were derived: H_2^{18}O : 94.12%; H_2^{16}O : 2.27%; H_2^{17}O : 0.85%; HD^{18}O : 0.41% and HD^{16}O : 0.011%. The decrease of the H_2^{18}O relative concentration from the stated value of the purchased sample (97 %) is due to the isotopic exchange between gas phase water molecules and normal water molecules adsorbed on the cell walls and in the admission tubes.

The self-continuum cross-section, C_s in $\text{cm}^2 \text{ molecule}^{-1} \text{ atm}^{-1}$, was determined as

$$C_s(\nu, T) = \frac{\alpha_c(\nu) k T}{P^2}, \quad (5)$$

3. Coherent Synchrotron Mode ($15\text{-}35 \text{ cm}^{-1}$)

3.1 Cross-section retrieval

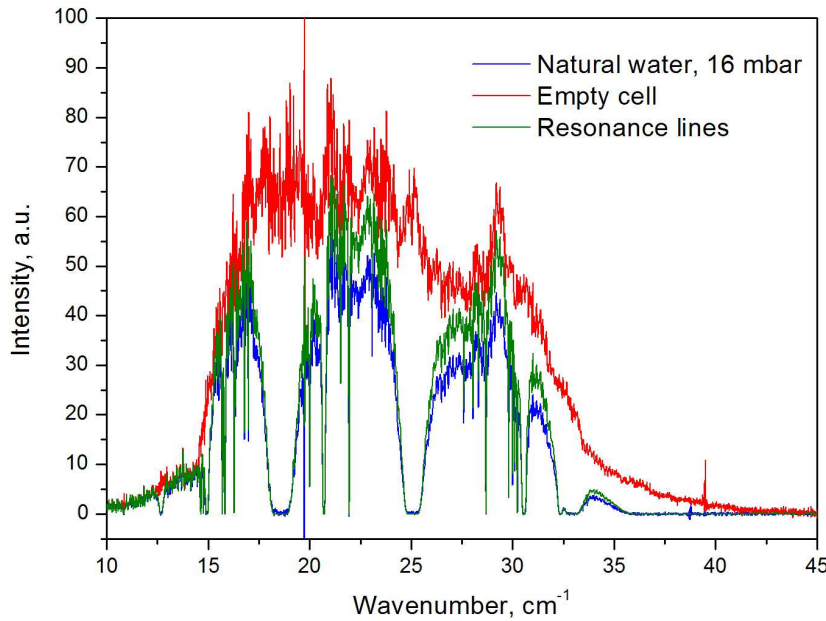


Fig.1.

Synchrotron power transmitted through the empty cell (red), cell filled with water (blue) and simulation corresponding to the resonance absorption only (green). The spectra were recorded with a 0.02 cm^{-1} resolution.

The coherent mode of the synchrotron radiation allows accessing the 15–35 cm⁻¹ range. **Fig. 1** presents a typical example of transmission spectra recorded with the cell filled with natural water vapor and with the empty cell (background spectrum). The water monomer spectrum simulation included in the figure was obtained as the product of the background spectrum with the transmittance factor calculated as described above. **Fig. 1** shows that the difference between the recorded spectrum and the simulation vanishes below 15 cm⁻¹ and above 35 cm⁻¹, indicating that the continuum measurements are not possible in those regions.

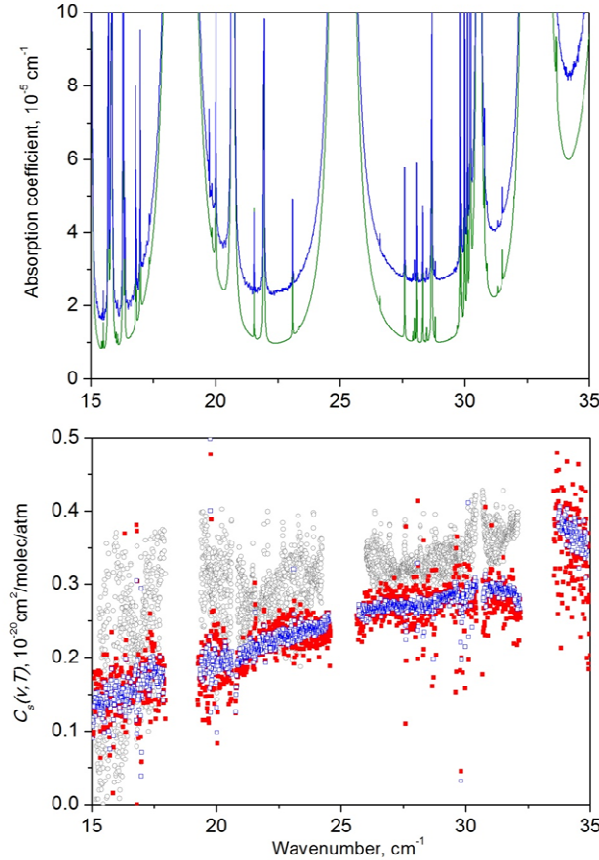


Fig.2.

Upper panel: FTS water vapor absorption spectrum recorded at 296 K and 16 mbar in natural isotopic abundance (blue), calculated water resonance absorption spectrum using the HITRAN2016 database [Gordon2016] (green).

Lower panel: Water vapor self-continuum cross-sections derived in this work from the 16 mbar (blue) and 11 mbar (red) recordings and comparison to the values derived in [Odintsova2017] from a spectrum recorded at 15.3 mbar from (grey). Missing values correspond to spectral intervals obscured by strong water lines (optical depth larger than 1.5).

The baseline stability of the spectra is a key criterion for continua retrieval. In the present recordings, the FTS stability was tested from a detailed analysis of several spectra recorded with the cell evacuated (baseline) and with the cell filled with 16 mbar of natural water vapor (sample spectrum). The background and water spectra were recorded successively four times each without any change in the spectrometer regime and data acquisition scheme. The very good coincidence of the series of recordings (down to the noise

level) confirmed the long-term stability of the experiment. The average of these four spectra was used for further continuum analysis.

The coincidence of the cross-section values derived from recordings at different pressures is another way to check both the baseline stability and the quadratic pressure dependence of the self-continuum which is a key test of the quality of the obtained results. Due to the limited beam time granted for these measurements, in addition to the 16 mbar recordings, FTS spectra could be recorded at a single additional pressure (about 11 mbar and 13 mbar for natural water and H_2^{18}O , respectively, roughly corresponding to a two times smaller continuum compared to 16 mbar). One hundred raw spectra were co-added for natural water at this pressure, which resulted in a somewhat lower SNR compared to the 16 mbar recordings (1520 raw spectra in total). However, the C_s values derived at 11 mbar and 16 mbar are found in very good coincidence as illustrated in **Fig. 2**. A similar agreement is achieved for the two sets of data acquired for ^{18}O -enriched water sample (**Fig. 3**, lower panel) confirming the square pressure dependence of the measured continua.

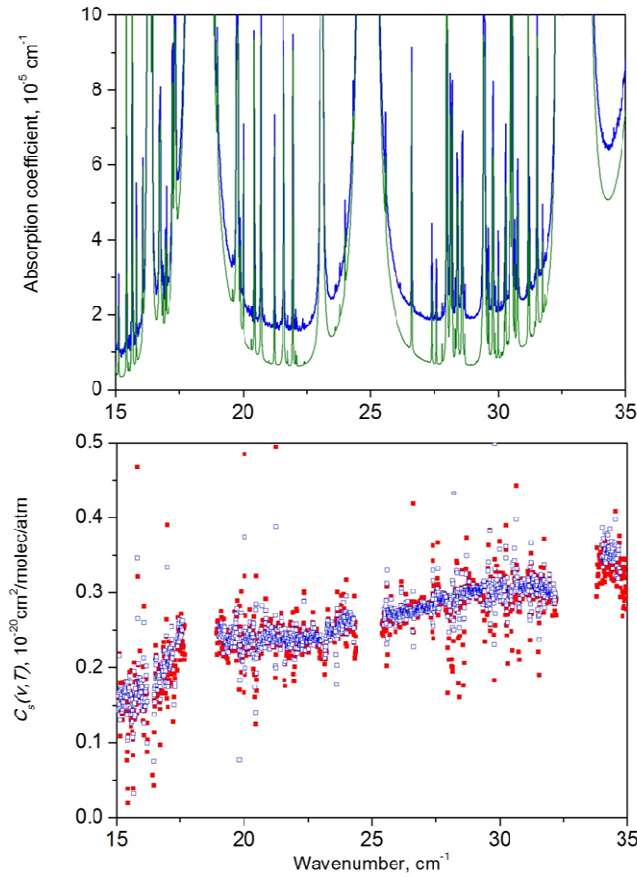


Fig.3.

Upper panel: FTS absorption spectrum of H_2^{18}O (94.1% enrichment) recorded at 296 K and 16 mbar (blue), corresponding water resonance absorption spectrum simulated using the HITRAN2016 database [Gordon2016] (green).

Lower panel: Water vapor self-continuum cross-section of H_2^{18}O derived from the 16 mbar (blue) and 13 mbar (red) recordings.

3.2 Comparison to literature data. Discussion.

Previous experimental studies of the water vapor self-continuum below 50 cm⁻¹ [Koshelev2011b, Kuhn2002, Slocum2015, Burch1982, Odintsova2017, Podobedov2008, Koshelev2018] are reviewed in **Table 2** which provides, for each of them, the experimental technique, spectral range and temperature conditions. An overview comparison of the literature results to the present measurements is presented in **Fig. 4**. In order to take into account the frequency dependence corresponding to the radiation term, the spectral function, $C_s(\nu)/\nu^2$ (also known as spectral density, spectral profile, spectral shape, [Frommhold2006, Hartmann2008]), is plotted. All the data correspond to 296 K. Continuum measurements for a number of temperatures (293, 313, 333 K) were performed in [Podobedov2008]. These data were recalculated to 296 K using the temperature exponent determined in [Podobedov2008].

The spectral function of the water dimer, (H₂¹⁶O)₂, included in **Fig. 4**, was calculated from the *ab initio* absorption spectrum presented in Fig. 8 from [Scribano2007]. Indeed, water vapor continuum in the 15-35 cm⁻¹ range is of particular interest since spectral signature of bound water dimer has been predicted in this region by *ab initio* [Scribano2007] and classical [Vigasin1983, Viktorova1970] calculations. Rotationally resolved water dimer spectrum at close to atmospheric conditions was recorded and unambiguously identified in the 3.5-8.5 cm⁻¹ range [Tretyakov2012, Serov2014, Koshelev2018]. Sequence of observed rotational peaks consists from a large number of overlapped lines (*E*-type transitions) corresponding to the end over end rotation of water dimer [Odintsova2014]. Peaks are observed separated by the dimer rotational constant $2B \sim 12.32$ GHz (≈ 0.4 cm⁻¹) [Fraser1989]. At room temperature, the sequence is supposed to reach a broad maximum located around 20 cm⁻¹. This maximum is predicted to be superposed to a broad absorption pedestal smoothly increasing with frequency, due to the overlapping of lines of *A*- and *B*-type transitions of bound water dimer (see e.g. Fig. 1 of [Odintsova2014]). In real water vapor similar smooth pedestal from quasibound states is expected. Such deviation of the water vapor continuum frequency dependence from a quadratic function (expected in earlier studies in mm [Koshelev2011b] and far IR [Podobedov2008] ranges) was tentatively evidenced in our preliminary work [Odintsova2017]. This conclusion relying on a single pressure recorded at 15.3 mbar (see Fig. 2 of Ref. [Odintsova2017]) is fully confirmed by the present results. In **Fig. 4**, the broad absorption maximum due to the dimer rotational absorption near 20 cm⁻¹ is transformed into a characteristic sharp slope of the spectral function. Our experimental data are found in very good agreement with the water dimer predictions in the 15-35 cm⁻¹ region. This confirms the dominant contribution of the water dimer absorption to the continuum in this region. Note the very good agreement with literature data, especially with quite reliable data recently reported by Slocum [Slocum2015] near 50 cm⁻¹ and unpublished results obtained by Bohlander within 14 microwindows of transparency in the range of 14-50 cm⁻¹ presented by Burch [Burch1982].

Let us underline that the water dimer contribution is dominating up to about 25 cm⁻¹ only. This is mostly due to the intense rotational spectrum of the dimer with a maximum around 15 cm⁻¹. In the range of maximum of the monomer rotational spectrum, the predicted dimer spectrum is mostly due to four low-lying fundamental vibrational bands (at about 88, 103, 108 and 143 cm⁻¹) and their multiple overtones and combination bands, all populated at room temperature. The resulting calculated spectrum is similar to the observed continuum [Scribano2007]. However, the relative importance of dimers decreases at higher wavenumbers. For example, in the 100-200 cm⁻¹ range, dimers are responsible for only about one half of the observed continuum [Odintsova2017, Serov2017] and far wings of monomer lines come into the play. In the millimeter-wave range (below about 10 cm⁻¹), far wings contribution to the spectral function is almost negligible because the monomer spectrum

maximum is located at about 150 cm^{-1} , far above the dimer rotational spectrum maximum. As detailed below, this is not the case in the $50\text{-}500\text{ cm}^{-1}$ interval studied with the standard synchrotron mode.

Table 2. Experimental conditions and techniques of previous continuum measurements.

Reference	Technique	T	Spectral interval, cm^{-1}
Burch1982	Interferometer	296	14-50 and 350-800
Kuhn2002	Resonator spectrometer	296-356	5.1-11.7
Podobedov2008	FTS	293-333	20-90
Koshelev2011b	Resonator spectrometer	261-328	3.5-4.8
Slocum2015	Video-spectrometer	296	50
Odintsova2017	FTS	297	14-35 and 40-200
Koshelev2018	Resonator spectrometer	296	3.5-8.5
This work	FTS	297	15-35 and 50-500

The MT-CKD values of $C_s(\nu)/\nu^2$ plotted in **Fig. 4** are mostly frequency independent up to 60 cm^{-1} . Although the MT-CKD average value is within the range of the observations, the frequency dependence is not reproduced. The MT-CKD empirical model is based on the assumption that the continuum originates from far wings of the monomer lines. It is thus not surprising that the MT-CKD predictions deviate from the observations in the considered spectral region where the dimer contribution dominates.

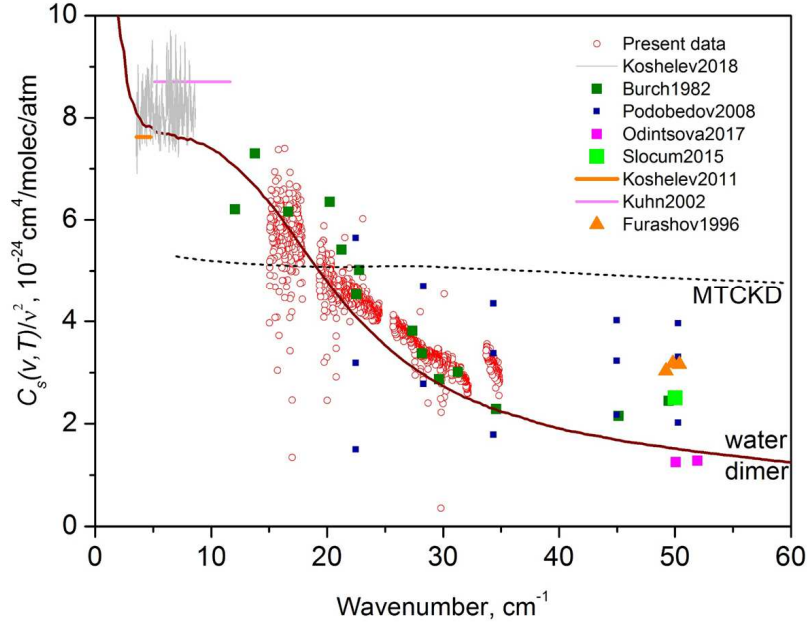


Fig. 4.

Overview comparison of the experimental values of the normalized self-continuum cross-section of water vapor, $C_s(\nu)/\nu^2$, to the spectral function of water dimer at room temperature (brown solid line) calculated *ab initio* [Scribano 2007] and the MT-CKD_3.2 model (dashed black line).

The lack of H_2^{18}O dimer spectrum calculations and previous experimental data on H_2^{18}O continuum prevents similar comparison for our H_2^{18}O data. The interaction potential of two water molecules being independent of the isotopologues, the H_2^{16}O and H_2^{18}O self-continua are expected to be close. This is confirmed by the comparison presented in **Fig. 5**. The coincidence within the experimental noise confirms the above mentioned non-quadratic frequency dependence of water vapor continuum in this spectral range. In principle a small isotopic shift to lower energy is expected for the heavier H_2^{18}O dimer. The end-over-end rotation spectrum of $(\text{H}_2^{18}\text{O})_2$ dimer can be roughly predicted shifted by about $1\text{-}2 \text{ cm}^{-1}$. However, the SNR of our data is not sufficient to evidence such small isotopic shift of the continuum.

We have plotted in **Fig. 5**, curves corresponding to a smoothing of the measured normalized self-continuum cross-sections. The corresponding values sampled with 0.5 cm^{-1} step are provided as Supplementary Material.

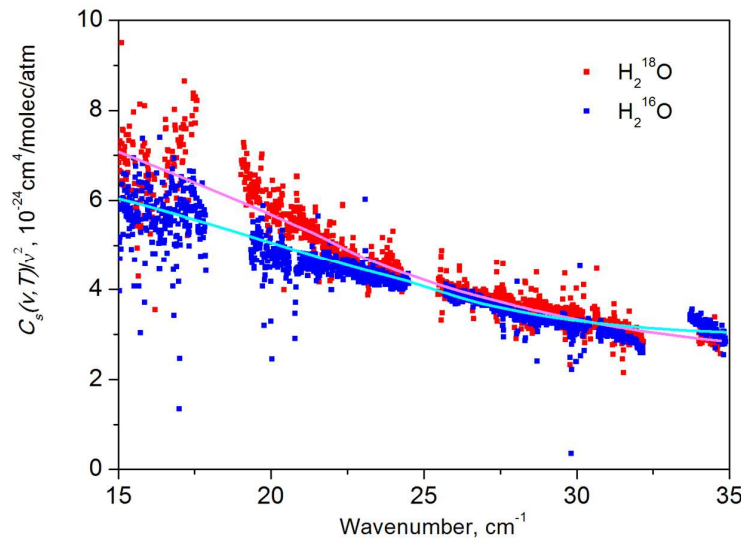


Fig. 5.

Comparison of H_2^{16}O and H_2^{18}O normalized self-continuum cross-sections, $C_S(v)/v^2$. Blue and red symbols correspond to H_2^{16}O and H_2^{18}O , respectively (both obtained from water vapor recording at 16 mbar). Light blue and magenta curves correspond to a smoothing of the H_2^{16}O and H_2^{18}O data, respectively.

4. Standard synchrotron mode (50-500 cm^{-1})

4.1 Cross-section retrieval

The standard mode of the SOLEIL synchrotron allowed for recording the H_2^{16}O and H_2^{18}O spectra in the 50-500 cm^{-1} range. The overview of the FTS spectrum of natural water is presented in **Fig. 6** together with the background spectrum recorded with the cell evacuated. Note the noisy appearance of the background spectrum. This quite regular spectral structure due to multiple interferences of radiation inside the spectrometer elements is very stable (see insert in **Fig. 6**) and thus strongly reduced when divided by the spectrum recorded with the water sample.

Two values of spectral resolution were chosen for the recordings (see **Table 1**). A first series consists of spectra recorded at intermediate resolution (0.02 cm^{-1} , ~ 30 minutes

acquisition time) with different water vapor pressures of natural and ^{18}O enriched water, between 2 and 6 mbar. This set of measurements allowed controlling the quadratic pressure dependence of the continuum. The second series consists of H_2^{16}O and H_2^{18}O spectra recorded with the maximum resolution (0.002 cm^{-1}) at about 3 and 6 mbar. These spectra allow investigating in detail the shape of continuum absorption, that is necessary for further analysis of its physical nature.

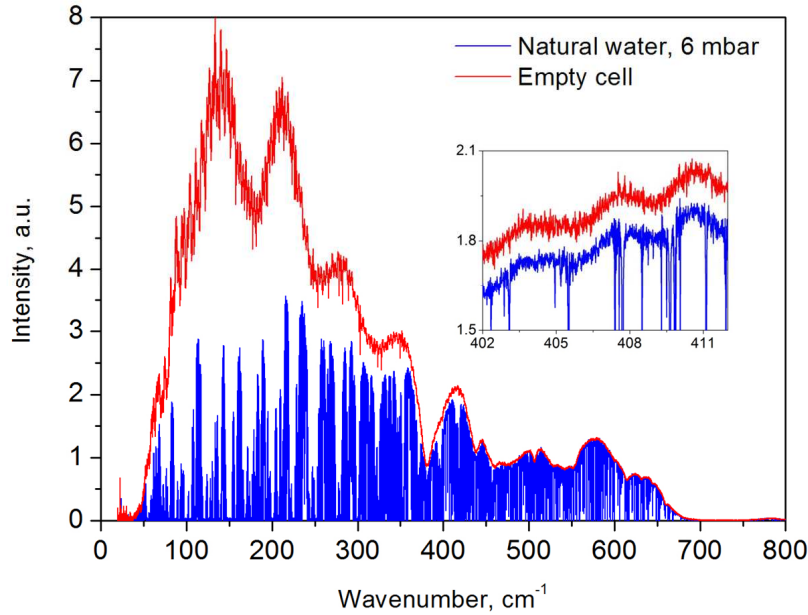


Fig. 6.

Transmission spectrum of natural water (blue) at a pressure of 6 mbar and corresponding background spectrum recorded with the empty cell (red).

The high intensity of the monomer transitions and the insufficient accuracy of individual line parameters (in particular for H_2^{18}O) prevented the global retrieval of the continuum by difference between the measured spectrum and the simulation of the monomer spectrum (Eq. 3). So, unlike to the $15\text{--}35 \text{ cm}^{-1}$ range, the continuum was determined only at about one hundred frequency points corresponding to micro-windows of transparency between resonance lines. At the chosen spectral points, the monomer contribution (up to 50% of the total measured absorption) was simulated on the basis of the HITRAN database and subtracted.

As illustrated in **Fig. 7** for a few of the chosen spectral points, a very good quadratic pressure dependence of the resulting absorption continuum is achieved. Self-continuum cross-sections and their statistical uncertainty were derived from a linear fit of the continuum absorption coefficient *versus* pressure squared (Eq. 6). The derived values for H_2^{16}O (118 points) and H_2^{18}O (127 points) are provided as Supplementary Material and plotted in **Fig. 8**. This data treatment was applied to the spectra recorded at resolution of 0.02 cm^{-1} for which about six pressure conditions were at disposal. The continuum cross-sections were also derived from the spectrum recorded at the highest resolution at a single pressure of 6 mbar and 4 mbar for H_2^{16}O and H_2^{18}O , respectively. The narrower instrumental function allowed

accounting better for the monomer contribution and thus enlarging the number of spectral points (about 6000). The C_S values obtained from the high resolution spectra are included in **Fig. 8**. They show an excellent agreement with the values derived from the pressure dependence analysis providing a mutual validation of the two approaches, in particular of the approximations concerning treatment of the apparatus function (see above).

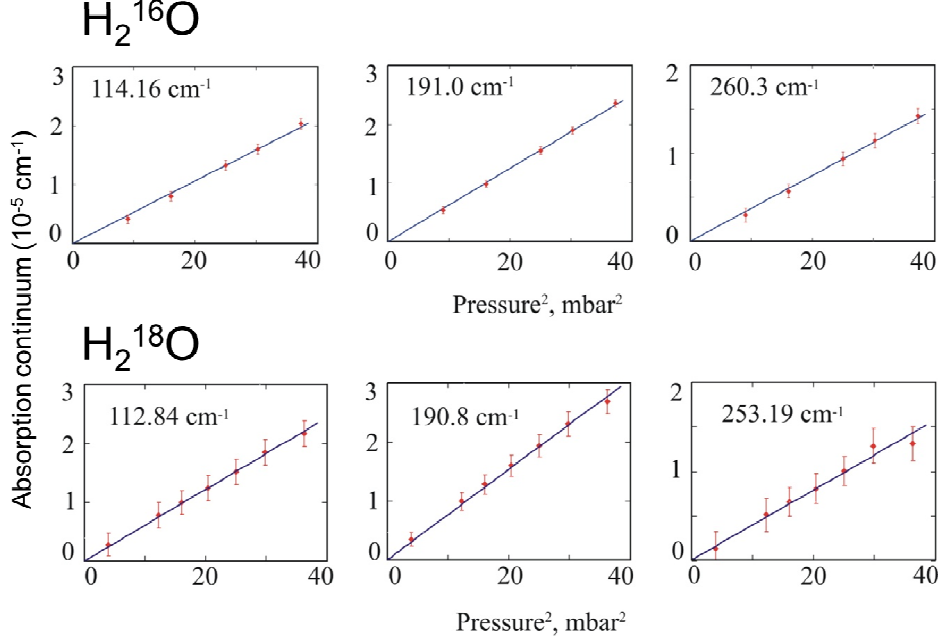


Fig. 7.

Continuum absorption coefficient of H_2^{16}O , (upper row) and H_2^{18}O (lower row) *versus* pressure squared in three selected micro-windows. Error bars correspond to one standard deviation of the noisy signal from its mean value within current micro-window.

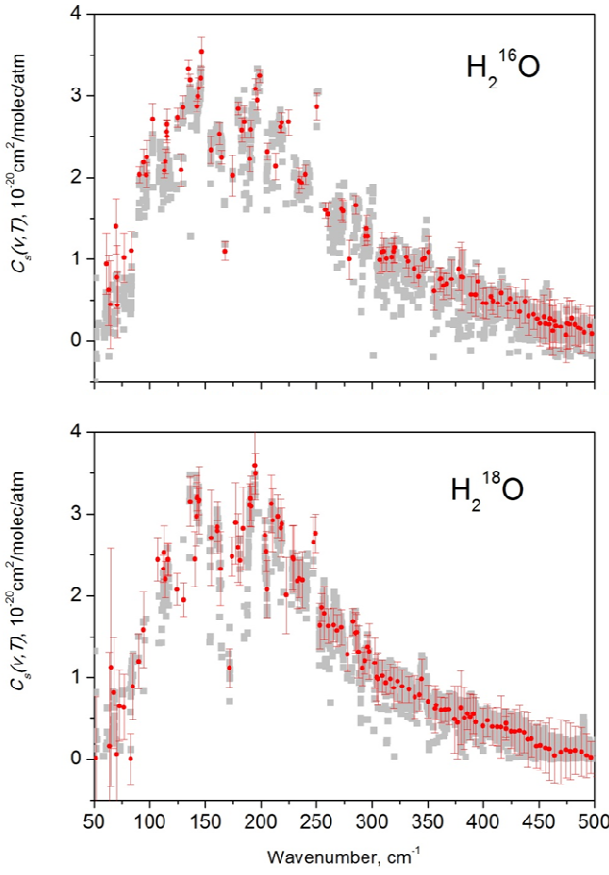


Fig. 8.

Self-continuum cross-sections of H_2^{16}O (upper panel) and H_2^{18}O (lower panel) retrieved from high resolution water vapor spectra at 4 mbar (grey squares). The red circles correspond to values derived from the analysis of the quadratic pressure dependence of the absorption in micro-windows selected in lower resolution recordings. Error bars correspond to one standard deviation of the noisy signal from its mean value within current micro-window.

4.2. Comparison to literature data. Discussion.

An overview of the literature data is presented in **Fig. 9** for natural water (see also **Table 2**). The new H_2^{16}O C_S values agree with our previous FTS measurements limited to the $40\text{-}200\text{ cm}^{-1}$ range [[Odintsova2017](#)]. The overall agreement with Burch above 350 cm^{-1} [[Burch1982](#)] is satisfactory although Burch's values are systematically larger than ours. The present measurements fill the $200\text{-}350\text{ cm}^{-1}$ gap where the water vapor continuum was not measured before. The data confirm that the widely used MT-CKD model [[Mlawer2012](#)] overestimates the continuum amplitude by a percentage between 30% and 100 % in the range of the rotational band of H_2O .

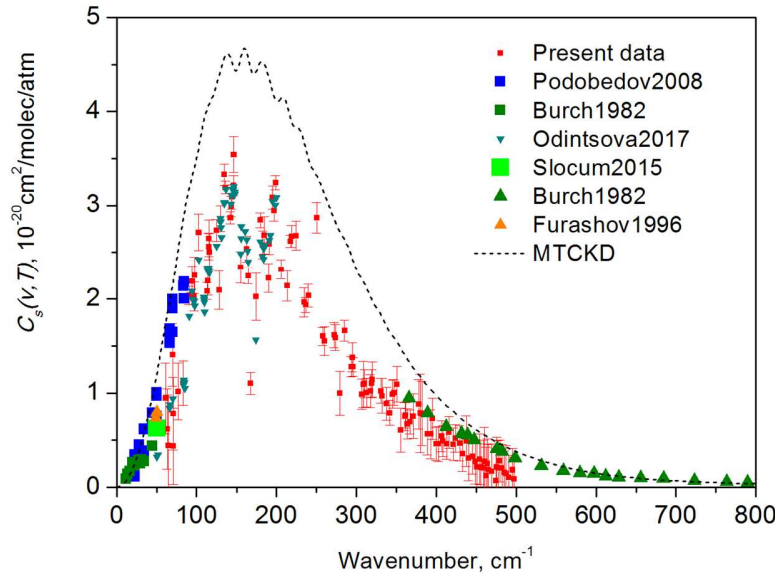


Fig. 9.

Comparison of the water vapor self-continuum derived in this work to previous experimental studies [Burch1982, Furashov1996, Odintsova2017, Podobedov2008, Slocum2015,] and to the MT-CKD_3.2 model [Mlawer2012].

As expected the H_2^{16}O and H_2^{18}O absorption continua are very similar in shape and magnitude (**Fig. 8**). We would like to point out and discuss the non-smooth frequency dependence of the H_2^{16}O and H_2^{18}O continua, which manifests itself as significant fluctuations of C_S values between nearby micro-windows. These fluctuations are reproducible and significantly larger than the experimental noise. Let us recall that the continuum involves contributions from monomolecular and bimolecular absorptions [Serov2017]. In our experimental conditions, the contribution of free molecular pairs is negligible [Vigasin1991]. So only bound and quasibound water dimers contribute to the bimolecular absorption and their contributions have a similar amplitude [Odintsova2017, Serov2017]. Regarding frequency irregularity of the dimer spectrum in our region the reader is referred to [Scribano2007] for results of quantum chemical calculations. Note that in [Scribano2007], the pressure broadening parameter value (0.12 cm^{-1}) used for computing the dimer spectrum was overestimated by about one order of magnitude [Serov2014]. Even though, one may see on Fig. 8 of [Scribano2007] that, within the $100\text{-}200 \text{ cm}^{-1}$ range, the dimer absorption shows some sharp irregular features with amplitude representing up to 10% of the unresolved broadband absorption. In our case, the bound dimer absorption should be superimposed on the contribution of the quasibound dimer which is broadened by metastable states lifetime. This should somewhat broaden the sharp structures in the total bimolecular spectrum. Nevertheless, taking into account the small water vapor pressure in our experiment, we cannot completely exclude the bimolecular absorption as a source of the observed irregular frequency dependence of the retrieved C_S values.

The subtraction of the resonance lines may also be responsible of the observed dispersion of the C_S values. Two mechanisms may contribute: (*i*) the uncertainty of line shape parameters taken from the HITRAN database (mostly the intensity and the self-broadening parameter) and (*ii*) inadequate resonance line shape modeling of the intermediate wings (at

about 5-10 cm^{-1} from the line center). In the following, we analyze the potential impact of both mechanisms.

In our region, the HITRAN database provides resonance line intensities with uncertainty ranging from 1 to 20%. However, it is believed that these error bars are conservative estimates and that the real uncertainty is about 1% [Conway2018, Birk2017], at least for the most intense lines. Such error bars have a marginal impact on the resonance absorption simulation and thus can hardly explain the observed non-smooth frequency dependence. On the contrary, the HITRAN uncertainty of the self-broadening parameter can be large (20%), even for some of the most intense lines. Possible impact of this uncertainty on the retrieved continuum was estimated from the following procedure:

(i) self-broadening parameter of all water lines were independently and randomly varied within the HITRAN uncertainty range and 80 sets of broadenings were generated for our line list;

(ii) water vapor absorption was simulated as the sum of the continuum and the resonance absorption, the first one was modeled as a smooth curve, that roughly reproduce our experimental data (blue curve in **Fig. 10**), and the second one was modeled as a line by line sum using their parameters from HITRAN database except for self-broadening parameters for which values as described in (i) were used;

(iii) the continuum spectra were determined by subtraction of the resonance absorption modeled using unperturbed HITRAN values from water vapor absorption data simulated at previous step (ii);

(iv) maximum and minimum values of the continuum obtained from the 80 statistically spread data at each selected absorption micro-window frequency were found. They are presented in **Fig. 10** (black curves) together with experimental data (red circles). This figure demonstrates that the line width uncertainty may lead to fluctuations from a smooth function with an amplitude comparable to the observations. The self-broadening coefficient of water lines is thus an important source in the error budget on C_s values.

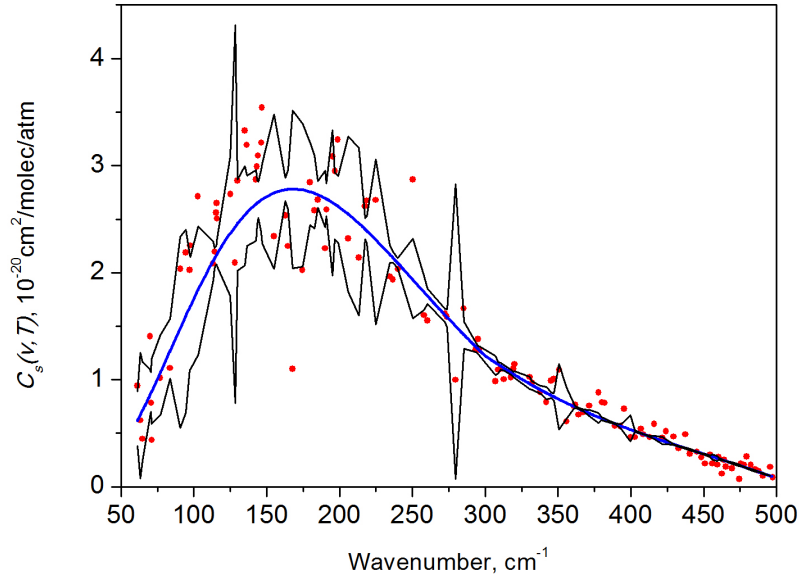


Fig. 10.

Estimated influence of the uncertainty of self-broadening parameters listed in HITRAN to the retrieved self-continuum cross sections (black curves), experimental values (red circles). The blue curve corresponds to a smoothing of the experimental values.

The impact of inadequate resonance line shape modeling (*i.e.* important deviations from the assumed line shape function), at large detuning from the line center was also considered. The total observed continuum absorption was approximated by a smooth function as before and a simple model was used to account for super- and sub-Lorentzian effects in the intermediate wings [Serov2017]. It is worth mentioning that practically the same approach was used in [Tran2017]. The model includes two variable parameters: the intermediate wing amplitude, A , and the characteristic width of the wing, $\Delta\nu_{wing}$. In [Serov2017], the best modeling of the continuum spectrum in the 40-200 cm⁻¹ range was achieved by setting the parameter $\Delta\nu_{wing}$ to 11 cm⁻¹, the value of the A parameter was determined from the fit of the continuum model to experimental data. The C_s values at the selected spectral points, calculated following this approach are plotted in **Fig. 11**. A negative correlation exists between the A and $\Delta\nu_{wing}$ parameters of the model: similar fit quality can be obtained by a simultaneous increase of $\Delta\nu_{wing}$ and decrease of A and *vice versa*. As expected, larger $\Delta\nu_{wing}$ values lead to a smooth cumulative contribution of the wings ($\Delta\nu_{wing}$) and smaller values of $\Delta\nu_{wing}$ entail irregular sharper structure similar to those observed in our experiment. This is illustrated in **Fig. 11** by two simulations corresponding to $\Delta\nu_{wing}$ equal to 88 and 5.5 cm⁻¹. Note that the smaller $\Delta\nu_{wing}$ value is more reasonable taking into account the mean collision duration between two water molecules evaluated in [Serov2017]. We thus conclude that uncertainties of intermediate and far line wings of the water resonance lines can also be a reason of the non-smooth frequency dependence of water vapor continuum.

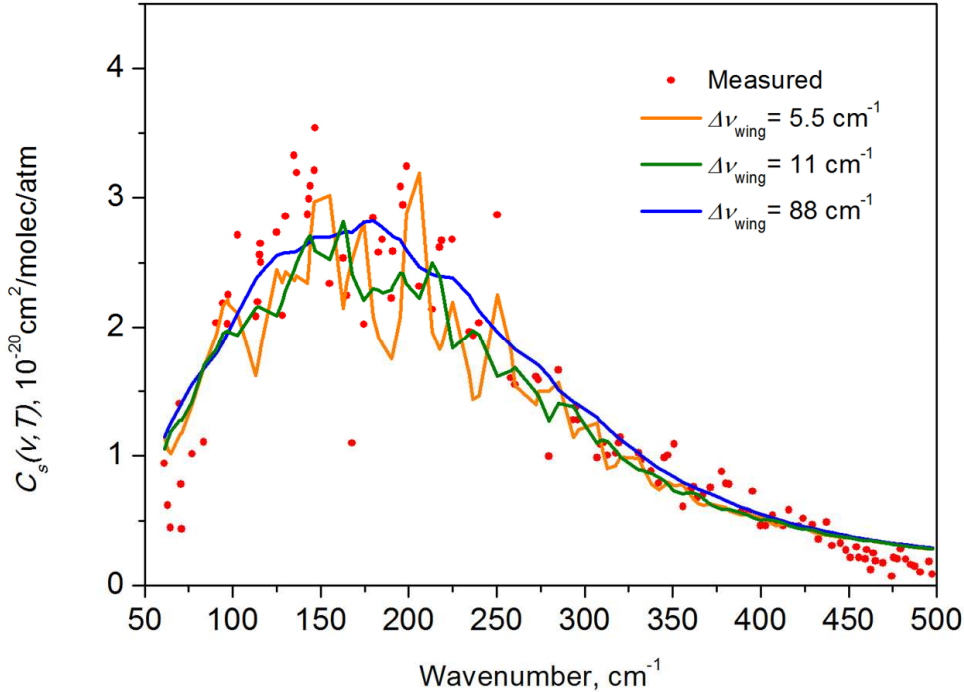


Fig.11.
Continuum model based on the line shape approach of [Serov2017] for different values of the $\Delta\nu_{wing}$ parameter and comparison to experimental continuum (red circles).

5. Conclusions

The self-continuum absorption of water vapor for the two main isotopologues (H_2^{16}O and H_2^{18}O) was investigated at the SOLEIL synchrotron in two frequency domains: $15\text{-}35 \text{ cm}^{-1}$ and $50\text{-}500 \text{ cm}^{-1}$. These spectral intervals are attractive for understanding the continuum origin by comparison to the unique quantum chemical calculations of the water dimer spectrum [Scribano2007]. To the best of our knowledge, the retrieved continua are the first ever reported for the H_2^{18}O isotopologue and for natural water in the $200\text{-}350 \text{ cm}^{-1}$ interval. The pressure squared dependence of the measured continua was systematically checked and used as criterion to validate the reported cross-section values.

The H_2^{16}O continuum in the $15\text{-}35 \text{ cm}^{-1}$ range together with literature results in the $3\text{-}50 \text{ cm}^{-1}$ range [Burch1982, Furashov1985, Kuhn2002, Podobedov2008, Koshelev2011b, Slocum2015, Odintsova2017, Koshelev2018] agree with *ab initio* calculations of the water dimer spectrum [Scribano 2007]. This agreement confirms the dominant contribution of water dimer absorption to the observed continuum in this domain. The SNR of the spectra and the absence of *ab initio* calculations of $(\text{H}_2^{18}\text{O})_2$ spectrum prevented to evidence the small isotopic red-shift of the H_2^{18}O continuum. The MT-CKD model does not account for the frequency dependence water self-continuum in this range.

The large $50\text{-}500 \text{ cm}^{-1}$ coverage of our spectra allows for comparison to various previous experimental investigations with more limited spectral coverage [Burch1982, Furashov1996, Podobedov2008, Slocum2015, Odintsova2017]. An overall general agreement is achieved for natural water while the MT-CKD model [Mlawer2012] significantly overestimates the continuum in this region. On the basis of spectra simulations, the inadequate description of the line shapes in the range of the intermediate wings (detuning of $5\text{-}10 \text{ cm}^{-1}$ from line center) and the uncertainties on the self-broadening coefficients of water monomer lines are identified as possible mechanisms responsible of the obtained irregular frequency dependence of the retrieved C_S values. The development of a more rigorous model of the intermediate line wings of water vapor appears to be a critical step to improve the analysis. In this context, the investigation of the isotopic dependence of the continuum in the rotational range may give insights to test the contribution of intermediate wings of resonance lines.

Acknowledgements

This work became possible due to the Project No 20180347 supported by SOLEIL Synchrotron Team. TAO, AOZ and MYT acknowledge Russian Foundation for Basic Research. The sub-THz range data treatment and the continuum retrieval was supported by project № 18-05-00698; the FIR data analysis was performed within the project № 18-02-00705; water dimer contribution in sub-THz range was analyzed within RAS program № 0035-2018-00002. PR and OP aknowledge partial support from CNRS-RFBR project 18-55_16006. The authors are grateful to C. Leforestier for numerical data related to *ab initio* calculations of water dimer absorption.

References

- [Birk2017] M. Birk, Wagner G, Loos J, Lodi L, Polyansky OL, Kyuberis AA, Zobov NF, Tennyson J. Accurate line intensities for water transitions in the infrared: Comparison of theory and experiment. *J Quant Spectrosc Radiat Transfer* 2017;203, 88–102.
- [Burch1982] Burch DE. Continuum absorption by H₂O. Report No AFGL-TR-81-03001982
- [Campargue2016] Campargue A, Kassi S, Mondelain D, Vasilchenko S, Romanini D. Accurate laboratory determination of the near infrared water vapor self-continuum: a test of the MT_CKD model. *J Geophys Res Atmos* 2016;121:13180–203. doi:10.1002/2016JD025531, 2016.
- [Clough1989] Clough SA, Kneizys FX, Davies RW. Line shape and water vapor continuum. *Atmospheric Research* 1989;23:229-41.
- [Conway2018] Conway EK, Kyuberis AA, Polyansky OL, Tennyson J, Zobov NF. A highly accurate *ab initio* dipole moment surface for the ground electronic state of water vapour for spectra extending into the ultraviolet. *J Chem Phys* 2018;149, 084307. doi:10.1063/1.5043545
- [Fraser1989] Fraser GT, Suenram RD, Coudert LH. Microwave electric-resonance Optothermal spectroscopy of (H₂O)₂. *J Chem Phys* 1989;90:6077–85.
- [Frommhold2006] Frommhold L. Collision-induced absorption in gases. Cambridge: Cambridge Univ. Press, 2006.
- [Furashov1996] Furashov NI, Sverdlov BA, Chernyaev SN. Absorption of electromagnetic radiation by pure water vapor at frequencies near 1.5 THz. *Radiophysics and Quantum electronics* 1996;39(9):754-9.
- [Golubiatnikov2005] Golubiatnikov GYu, Shifting and broadening parameters of the water vapor 183-GHz line (313-220) by H₂O, O₂, N₂, CO₂, H₂, Ne, Ne, Ar and Kr at room temperature. *J Mol Spectrosc* 2005;230:196-8.
- [Golubiatnikov2006] Golubiatnikov GYu, Markov VN, Guarneri A, Knoechel R. Hyperfine structure of H₂¹⁶O and H₂¹⁸O measured by lamb-dip technique in the 180-560 GHz frequency range. *J Mol Spectrosc* 2006;240:251-254.
- [Golubiatnikov2008] Golubiatnikov GYu, Koshelev MA, KrupnovAF. Pressure shift and broadening of water vapor lines by atmosphere gases. *J Quant Spectrosc Radiat Transf* 2008;109:1828–33.
- [Gordon2016] Gordon IE, Rothman LS, Hill C, Kochanov RV, Tan Y, Bernath PF, et al. The HITRAN2016 molecular spectroscopic database. *J Quant Spectrosc Radiat Transfer* 2017;203:3-69.
- [Hartmann2008] Hartmann JM, Boulet C, Robert D. Collisional effects on molecular spectra: laboratory experiments and models, consequences for applications. Amsterdam: Elsevier, 2008.
- [Koshelev2007] Koshelev MA, Tretyakov MYu, Golubiatnikov GYu, Parshin VV, Markov VN, Koval IA. Broadening and shifting of the 321-, 325- and 380-GHz lines of water vapor by the pressure of atmospheric gases. *J Mol Spectrosc* 2007;241;101-8.
- [Koshelev2011a] Koshelev MA. Collisional broadening and shifting of the 211–202 transition of H₂¹⁶O, H₂¹⁷O, H₂¹⁸O by atmosphere gases. *J Quant Spectrosc Radiat Transfer* 2011;112:550–2.
- [Koshelev2011b] Koshelev MA, Serov EA, Parshin VV, Tretyakov MYu. Millimeter wave continuum absorption in moist nitrogen at temperatures 261–328 K. *J Quant Spectrosc Radiat Transfer* 2011;112:2704–12.
- [Koshelev2018] Koshelev MA, Leonov II, Serov EA, Chernova AI., Balashov AA, Bubnov GM, Andriyanov AF, Shkaev AP, Parshin VV, Krupnov AF, Tretyakov MYu. New frontiers in modern resonator spectroscopy, 2018;8(6):773-783. DOI:10.1109/TTHZ.2018.2875450

- [Lechevallier2018] Lechevallier L, Vasilchenko S, Grilli R, Mondelain D, Romanini D, Campargue. The water vapour self-continuum absorption in the infrared atmospheric windows: new laser measurements near 3.3 and 2.0 μm . *Atmos Meas Tech* 2018;11, 2159–2171. doi.org/10.5194/amt-11-2159-2018.
- [Mlawer2012] Mlawer EJ, Payne VH, Moncet JL, Delamere JS, Alvarado MJ and Tobin DC. Development and recent evaluation of the MT_CKD model of continuum absorption. *Phil Trans R Soc A* 2012;370:2520–56.
- [Odintsova2014] Odintsova TA, Tretyakov MYu, Krupnov AF, Leforestier C. The water dimer millimeter-wave spectrum at ambient conditions:a simple model for practical applications. *J Quant Spectrosc Radiat Transf* 2014;140:75–80.
- [Odintsova2017] Odintsova TA, Tretyakov MY, Pirali O, Roy P. Water vapor continuum in the range of rotational spectrum of H_2O molecule: new experimental data and their comparative analysis. *J Quant Spectrosc Radiat Transf* 2017;187:116–23.
- [Podobedov2008] Podobedov VB, Plusquellec DF, Siegrist KE, Fraser GT, Ma Q, Tipping RH. New measurements of the water vapor continuum in the region from 0.3 to 2.7 THz. *J Quant Spectrosc Radiat Transfer* 2008;109:458–67.
- [Richard2017] Richard L, Vasilchenko S, Mondelain D, Ventrillard J, Romanini D, Campargue A. Water vapor self-continuum absorption measurements in the 4.0 and 2.1 μm transparency windows. *J Quant Spectrosc Radiat Transf* 2017;201:171–9.
- [Scribano2007] Scribano Y, Leforestier C. Contribution of water dimer absorption to the millimeter and far infrared atmospheric water continuum. *J Chem Phys* 2007;126:234301
- [Serov2014] Serov EA, Koshelev MA, Odintsova TA, Parshin VV, Tretyakov MYu. Rotationally resolved water dimer spectra in atmospheric air and pure water vapour in the 188–258 GHz range. *Phys Chem Chem Phys* 2014;16(47):26221–33.
- [Serov2017] Serov EA, Odintsova TA, Tretyakov MY, Semenov VE. On the origin of the water vapor continuum absorption within rotational and fundamental vibrational bands. *J Quant Spectrosc Radiat Transf* 2017;193:1–12.
- [Shine, 2012] Shine KP, Ptashnik IV, Rädel G. The water vapour continuum: brief history and recent developments. *Surv Geophys* 2012;33:535–55.
- [Slocum2015] Slocum DM, Giles RH, Goyette TM. High-resolution water vapor spectrum and line shape analysis in the terahertz region. *J Quant Spectros Radiat Transfer* 2015;159:69–79.
- [Tran2017] Tran H, Li G, Ebert V, Hartmann JM. Super- and sub-Lorentzian effects in the Ar-broadened line wings of HCl gas. *J Chem Phys* 2017;146:194305. doi:10.1063/1.4983397
- [Tretyakov2012] Tretyakov MN, Serov EA, Koshelev MA, Parshin VV, Krupnov AF. Water dimer rotationally resolved millimeter-wave spectrum observation at room temperature. *Phys Rev Lett* 2013;110:093001.
- [Tretyakov2013] Tretyakov M Yu, Koshelev MA, Vilkov IN, Parshin VV, Serov EA. Resonator spectroscopy of the atmosphere in the 350–500 GHz range. *J Quant Spectrosc Radiat Transfer* 2013;114:109–21.
- [Vigasin1983] Vigasin AA, Chlenova GV. The rotational spectrum of $(\text{H}_2\text{O})_2$ at atmospheric conditions. *Izv Akad Nauk SSSR. Fiz Atmos Okeana* 1983;19:703 (in Russian).
- [Viktorova1970] Viktorova AA, Zhevakin SA. Rotational spectrum of water-vapor dimer. *Sov Phys Dokl* 1971;15:852, Translated from: *Dokl. Akad. Nauk SSSR* 194 540 (1970).
- [Vigasin1991] Vigasin AA. Bound, metastable and free states of bimolecular complexes. *Infrared Phys.* 1991;32:461-70.